Structural evolution of the Pb/Si(111) interface with metal overlayer thickness

Jaime Souto-Casares, Tzu-Liang Chan, James R. Chelikowsky, Kai-Ming Ho, Cai-Zhuang Wang, and S. B. Zhang

Phys. Rev. B **92**, 094103 — Published 11 September 2015

DOI: 10.1103/PhysRevB.92.094103

Structural evolution of the Pb/Si(111) interface with metal overlayer thickness

Jaime Souto-Casares[1], Tzu-Liang Chan[1,2,3], James R. Chelikowsky[1,4], Kai-Ming Ho[5,6], Cai-Zhuang Wang[5], and S. B. Zhang[2]
[1] *Center for Computational Materials, Institute for Computational Engineering and Sciences, University of Texas at Austin, Austin, Texas 78712, USA,* [2] *Department of Physics, Applied Physics, and Astronomy, Rensselaer Polytechnic Institute, Troy, New York 12180, USA,* [3] *Department of Physics, Hong Kong Baptist University, Hong Kong,* [4] *Departments of Physics and Chemical Engineering, University of Texas at Austin, Austin, Texas 78712, USA,* [5] *Ames Laboratory - U. S. Department of Energy, Ames, Iowa 50011, USA,* [6] *Department of Physics and Astronomy, Iowa State University, Ames, Iowa 50011, USA.*

We a employ real-space pseudopotential method to compute the structural energies of a prototypical system metal-semiconductor interface. Specifically, we examine a Pb(111) film overlaid on a Si(111) substrate as a function of the metal thickness. For each layer of Pb we fully relax the atomic coordinates and determine the lowest energy structure. Owing to the lattice mismatch between the Pb and Si crystal structures, we consider a large supercell containing up to 1,505 atoms for the largest system. Systems of this size remain challenging for most current computational approaches and require algorithms specifically designed for highly parallel computational platforms. We examine the structural properties of the interface with respect to the thickness of the metal overlayer, *e.g.*, the corrugation of the profile of the Pb overlayer. The combined influence of the Si substrate and quantum confinement results in a rich profile for a transition between a thin overlayer (less than a few monolayers) where the corrugation is strong, and the bulk region, (more than a half dozen layers) where the overlaid Pb film is atomically flat. This work proves the feasibility of handling systems with such a level of complexity.

PACS numbers: 61.46.w, 68.35p, 81.07.-b

I. INTRODUCTION

The study of ultra thin metal films interfaced with a semiconductor substrate is technologically important owing to the ubiquitous nature of metal-semiconductor contacts in electronic devices. The study of such interfaces is also also important because of the role that quantum confinement plays in such systems as devices approach the nanoscale.[1–3] Confining electrons within a thin film can result in oscillations in the work function of the metal film,[4], and the emergence of anomalous superconducting effects.[5] Moreover, the advent of new techniques for epitaxial depositing permits experimental groups to routinely grow and control ultra thin films at atomic level and observe such effects. It has been discovered that metal atoms can be arranged into well defined islands of particular heights on a semiconductor substrate, and this behavior can be dominated by quantum confinement.[6] This effect has been observed in interfaces, such as Ag/GaAs(110),[7] Ag/Si(111),[8] Pb/Ge(111),[9] and also Pb/Si(111).[10,11]

Among other metal-semiconductor systems, the latter has been granted special attention. Pb under certain circumstances can form an atomically abrupt interface with Si forming a distinct metal semiconductor interface.[12] For this reason, we focus on the Pb/Si interface. While the interface can be abrupt, the details of the interfacial geometry can be complex. The interface structure can display a (7×7) phase,[13] the β-$(\sqrt{3} \times \sqrt{3})$R30°[12] and the *mosaic*-$(\sqrt{3} \times \sqrt{3})$R30° phase,[14] the (1×1) phase,[15] or the hexagonal[16] and stripe incommensurate phases.[17] In order to navigate through this complexity, theoretical and computational analysis can complement, support, and even suggest experimental activity. However, the computational study of an atomistic Pb/Si(111) interface presents several challenges, mostly related with the size of the system. Systems with more than ∼1,000 atoms are not tractable for current computational methods, especially when we compute forces and relax the surface. Strong experimental evidence exists that structural relaxation of the interface is required for a correct description of its electronic properties (*e.g.*, see Ref. [18] and references therein).

After deposition of 3 monolayers of Pb onto a Si(111) substrate, LEED experimental measures of the interface show Moiré patterns with wavelengths of 35 Å.[19] These patterns can be related to the lattice mismatch between the Pb(111) and Si(111) surfaces, imposing a minimum size for the lateral dimension of the unit cell. The lattice constant of Si (5.43 Å) and that of Pb (4.95 Å) dictate the number of atoms considered in the calculation (81 Si and 100 Pb per layer). Electronic structure computations for this problem can be formidable. Ten overlayers of Pb would result in a 1,000 Pb atom system wherein each Pb atom should be moved until an equilibrium configuration is achieved. The use of fast and efficient computational methods and state of the art hardware are mandatory to

make progress for such a system. Historically, quantum based calculations have not been practical for such systems without some notable approximations, such as the jellium model where the atomic positions are not considered, or the use of small unit cells that does not match the experimental lattice mismatch between the metal and semiconductor semi-slabs.[20–25]

Here, we study the evolution of the Pb/Si(111) interface with the metal coverage by means of computer simulation, with our focus on structural properties. Some effort has been put into detailing the computational methods used to perform the calculations in Sec. II. The real-space approach along with specialized algorithms and an optimal implementation of the periodicity of the system allows us to access very large systems. In Sec. III, the discussion is focused on the construction of the Pb(111)/Si(111) interface. The accurate treatment of the lattice mismatch between both parts if the interface, key for a correct characterization of the system, is addressed here. Sec. IV presents the results and analysis of different geometrical and energetic properties of interest. Finally, some conclusion are discussed in Sec. V.

II. COMPUTATIONAL METHOD

Our calculations were performed using PARSEC,[26–28] a real-space implementation of pseudopotentials within density functional theory.[29,30] PARSEC solves the Kohn-Sham equations self-consistently on an orthogonal, uniform, three-dimensional grid on real-space. Real-space methods have a number of advantages in terms of computer performance with respect to plane-wave methods, which have been traditionally the most popular approach. First, a real space description possesses inherent semi-locality, which makes them well suited for massive parallelization as global communications among processors are minimized. Second, boundary conditions are flexible: they can be either periodic or confined. For the latter, wave functions and potentials are required to vanish beyond certain distance. Appropriate usage of boundaries allows for the trimming of the simulation boxes, thus reducing the computational cost. We use high order finite differencing to express the Laplacian operator. Typically, 6th to 8th order finite difference expressions are used. Finite differing methods offer ease of implementation when compared to other real space methods, *e.g.* , finite elements.

Solving the Kohn-Sham equations consists of the diagonalization of the Hamiltonian matrix, which in real-space takes the form of a highly sparse matrix. Very efficient iterative solvers are available to attack this problem, such as ARPACK [31] or TRLanc,[32] both implemented in PARSEC. More recent version of PARSEC replace exact diagonalization with a subspace filtering iteration via Chebyshev polynomials.[33,34] Instead of applying the eigensolver in every cycle of the self-consistent loop, one only needs to perform it once at the beginning of the calculation in order to get a good initial basis, and the filter will iteratively improve the solution. The improvement attained by this method has been found to lie around one order of magnitude, allowing the examination of much larger systems than traditional methods.[33,34]

The local density approximation of Ceperley and Alder[35] was used for the exchange-correlation potential as parametrized by Perder and Zunger.[36] The ion core potentials were represented by norm-conserving pseudopotentials using the Troullier-Martins prescription,[37] with reference configuration $[Xe]6s^26p^26d^0$ and $[Ne]3s^23p^23d^0$ for Pb and Si respectively. Scalar relativistic effects were taken into account in the construction of the Pb pseudopotential.[37] The distance between adjacent point in the real-space grid was 0.66 a.u., which ensures energy convergence of the system. We sample the Brillouin zone at the Γ point. Given the large size of the unit cell, the Γ point offers a effective sampling of the charge density.

III. MODELING THE Pb/Si INTERFACE

Our Si pseudopotential yields a lattice constant of 5.39 Å, and our Pb pseudopotential yields a lattice constant of 4.85 Å, both values are about 1-2% smaller than experiment. As a consequence, the Si substrate and Pb film are minimally strained within our calculation as $5.39\times9 \approx 4.85\times10$. This pattern is consistent with experiment.[19] The Pb pseudopotential used in our work also reproduces the minima and maxima of the surface energy of free-standing Pb films as found in previous work.[38]

A 4-layer Si substrate with the surface structure a (1×1) relaxation is put in contact with a Pb slab made by films with thickness ranging from 1 up to 11 layers. The interface is aligned matching the $(1\bar{1}0)$ direction of both the Si substrate and the Pb overlayer. Our interface contains a (9×9) unit cell for the Si, and the Pb overlayer composed of films with 10×10 atoms per layer. An additional layer of H atoms is placed on the bottom side of the Si substrate to saturate the dangling bonds. A mixed boundary condition scheme was used to construct the simulation box: periodic along the slab normal plane, and confined along the perpendicular axis, which removes the problem of replica interactions.[28] A vacuum space of 8 Å is left for the wave functions to decay above the Pb side, while 4 Å is enough for the H passivation layer. Every Pb atom and the first bilayer of Si are allowed to fully relax until the force on each atom was less than 0.005 Ryd/a.u. An atomic model of Pb/Si interface is illustrated in Fig. 1(a). For the largest model studied, 1,100 Pb atoms were included on top of the 405 Si and H atoms. In order to validate whether our 4-layer Si plus H-passivation is sufficient to model a semi-infinite substrate, we have checked that the inclusion of one and two additional double layers of Si. We found this inclusion has no impact on the structural details of the interface.

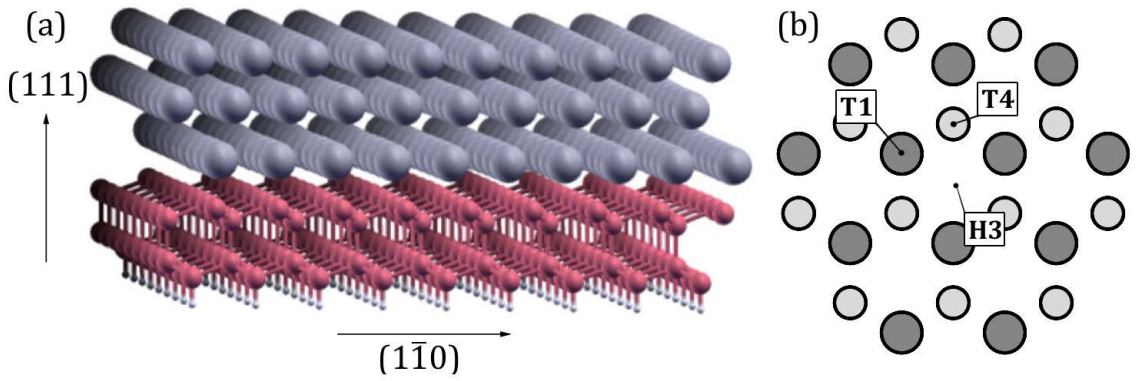

FIG. 1: (a) Atomic model of the unit cell for a Pb/Si junction: a three layer Pb(111) film on a 4-layer Si(111) substrate passivated by H atoms at the bottom. (b) Schematic plane projection of a portion of a Si bilayer. Larger and darker points represent the upper layer, and the smaller and brighter the bottom one. The special sites of the surface, T1, T2, H3, are shown.

IV. RESULTS AND DISCUSSION

Each layer must be fully relaxed to obtain the lowest energy structure. We find that both the Si substrate and the Pb overlayer remain bulk-like in terms of the atomic coordination, which is consistent with experimental observations[19,39]. However, there are notable corrugations in the Pb film for a few monolayer coverages. For each atomic layer of the Pb film, the corrugation is obtained by taking the difference in height between the lowest and highest atom in the layer. The Pb film is not atomically flat and reflects an undulation of ∼0.1 Å. In Fig. 2, we illustrate the corrugation of each atomic layer in an 11-layer thick Pb film on Si. The corrugation originates from the Pb/Si interface, decays strongly after a maximum at the second layer, and then propagates to the top of the Pb film with strain. A Pb atomic layer is essentially flat seven to eight layers away from the interface;

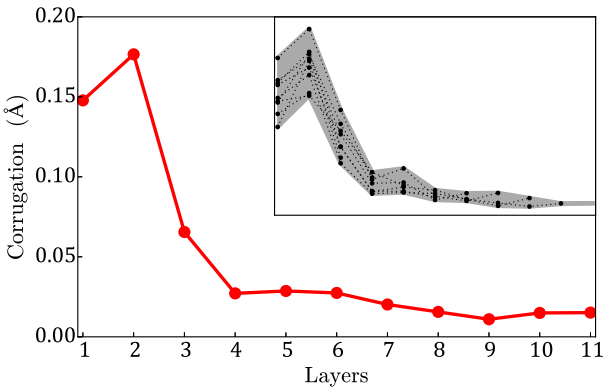

FIG. 2: Layer-by-layer corrugation profile for an optimized 11-layer thick Pb film on Si(111). The first layer is just above the Si substrate, and the last layer at the top of the Pb film. The inset shows the corrugation profile for all of the interfaces calculated, ranging from 3-layer to the 11-layer Pb film. Both graphs share the same axes.

the influence of the Pb/Si interface on Pb film extends for ∼6 Pb atomic layers. Moreover, this general behavior does not depend on the thickness of the Pb overlayer. This is shown in the inset of Fig. 2, where the gray area encloses the level of corrugation for the different Pb overlayer thickness.

Fig. 3 shows the corrugation profile for every layer in the 11-layer thick Pb film, including the Si layer in contact with the interface (bottom right corner). A major factor shaping these profiles is the location of the special sites above the Si substrate, in particular the position of these sites with respect to the atoms that form the bottom Pb film. As it can be seen in Fig 2(b), T1 and T4 represent the top site of the upper and lower half of the first bilayer of Si, respectively, while H3 indicates the hollow site. The location of these sites with respect to our unit cell is shown in the bottom-mid panel of Fig. 3. The first three layers of Pb, where the corrugation is most notable, present a simple topology, with a well localized maximum on the T1 site, and a more disperse minimum, centered on the H3 site that stretches towards the T4 site. The pattern becomes more intricate after the forth layer, where the number of local extrema within the local cell grows and the level contours start to display more oscillations. At this height, the level of corrugation has decreased, but films 4, 5, and 6 still retain some influence from the Si substrate as the global maximum and minimum corrugation points are located in special sites. For instance, layer 6 presents maximum and minimum corrugation on the H3 and T4 site, respectively. The thickest films of Pb, with corrugations $\lesssim 0.02$ Å, evolve towards a map with well localized maxima and minima arranged in a triangular tiling, resembling the map from the first Pb layer, but where the location of the extrema are no longer determined by the special sites. In short, the corrugation profile for the middle layers can be seen as a transition between two regimes, one close to the Si substrate and therefore determined by it, and one far from the substrate, where this influence is mostly suppressed. Although these general trends are followed by

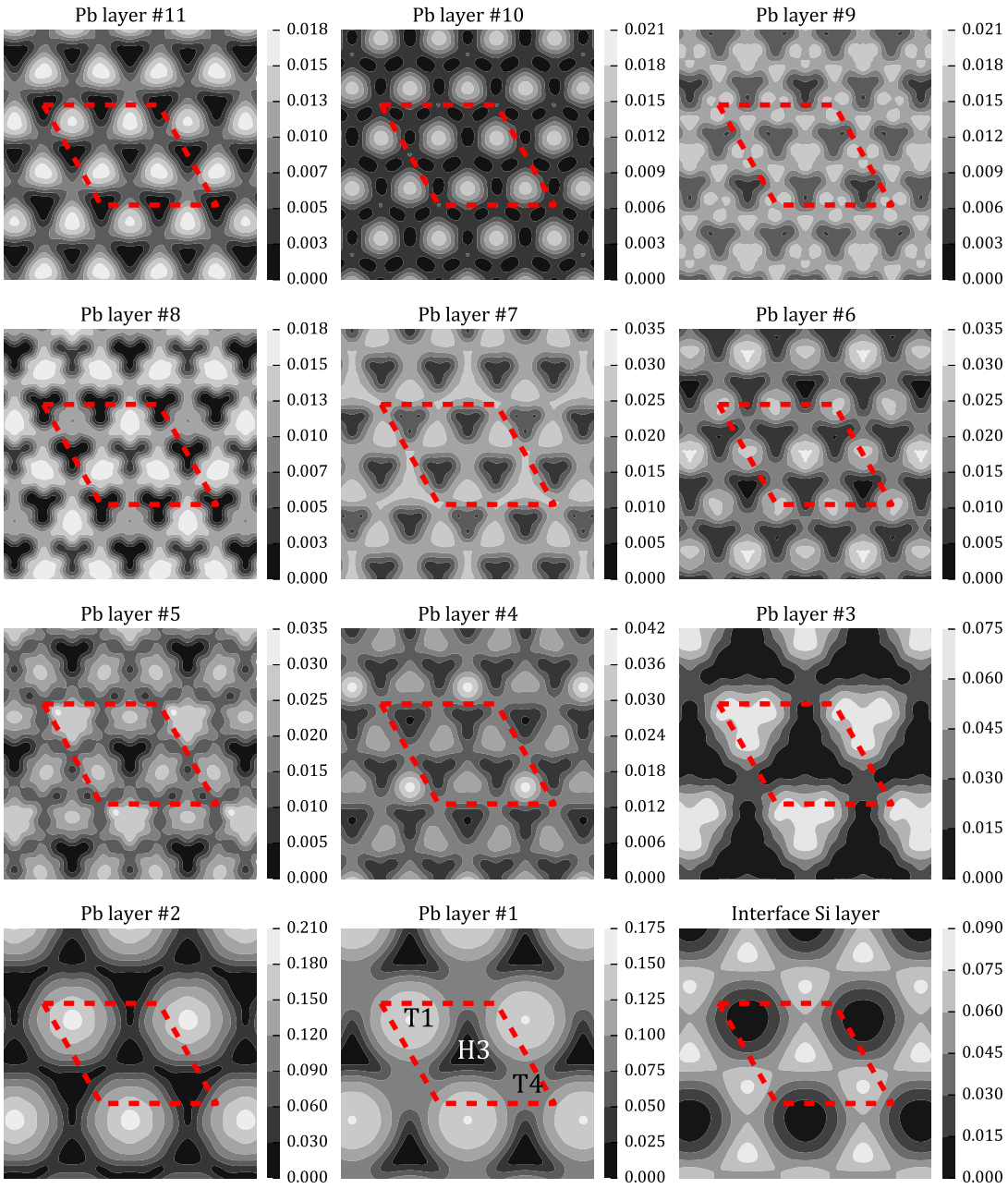

FIG. 3: Corrugation profiles (units of Å) for the 11 layers of Pb in a thick Pb/Si interface, together with the profile for the Si layer in contact with the Pb overlayer (bottom-right panel). Dashed red line shows the unit cell, whose side length is 34.3 Å. For the sake of better readability, T1, T4 and H3 points for the bottom Pb film are only displayed in the bottom-mid panel.

all the systems regardless of their overlayer thickness, we have found that the particular corrugation map for each layer in the middle part of the overlayer change depending on the amount of overlying lead. It is also notable that, specially for the systems with at least a few Pb overlayers the pattern displayed onto the unit cell could not be divided into smaller replicas, *i.e.*, a smaller unit cell cannot be constructed to capture the evolution of the corrugation profile.

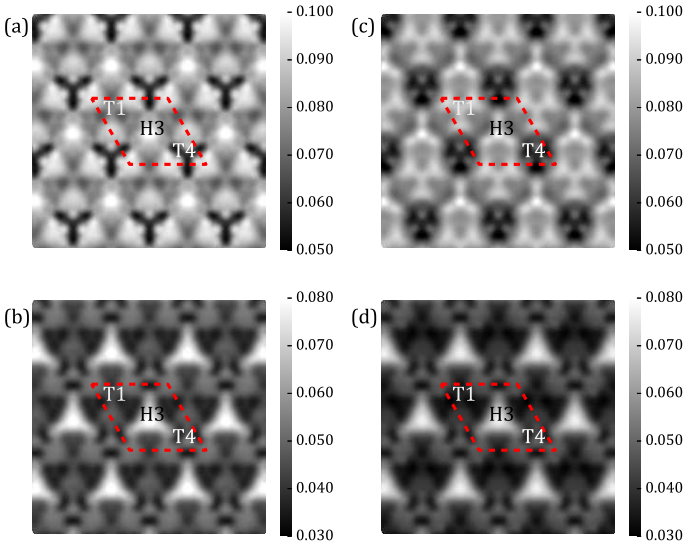

FIG. 4: Thickness profile of the three layer Pb film on Si(111) for different Pb overlayer thickness with respect to an unrelaxed three layer Pb film (units of Å). (a) 4 layer-thick, (b) 5 layer-thick, (c) 10 layer-thick, and (d) 11 layer-thick. Dashed red line represents the unit cell, whose side length is 34.3 Å. Special sites of the Si substrate (T1,T4, and H3) with respect to the Pb film in contact are shown.

The Pb film does not have a uniform thickness either. The thickness profile of a three layer Pb film next to the Si substrate for different Pb overlayer thickness is shown in Fig. 4. The magnitudes are referenced to the thickness of a film with 3 unrelaxed layers of Pb. The upper pair, Fig. 4(a) and Fig. 4(b), corresponds to the 4- and 5-thick layer Pb, respectively. These maps show a notable thickness enlargement, with the maximum point located on top of the H3 site, and a clear area where the thickness reaches its minimum around the T4 site. This situation changes drastically for the thicker overlayers in the lower pair, with 10, Fig. 4(c), and 11, (d), layers of Pb. The hollow site remains as the point of maximum thickness. However, the dominant shade in the map has changed over to dark gray, meaning that the stacking of Pb films leads to a weaker strain along the slab axis.

It is difficult to grow such thin atomically flat, yet stable, Pb films at all coverages. To see this, we compute the stability of Pb(111) films on Si(111) substrate by examining the formation energy

$$E_{form} = E - E_{sub} - n_{Pb} \times \mu_{Pb}, \qquad (1)$$

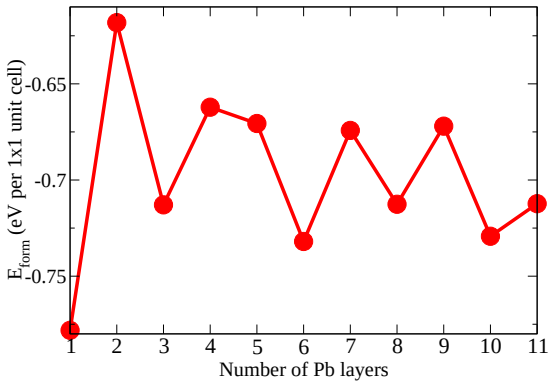

FIG. 5: The formation energies E_{form} of Pb films on Si(111).

where E is the energy of the Pb/Si system, E_{sub} is the energy of the Si(111) substrate without the Pb overlayer, n_{Pb} is the number of Pb atoms in the system, and μ_{Pb} is the chemical potential of Pb. In our calculations, μ_{Pb} adopts the energy of a Pb atom in its bulk face centered cubic structure. The calculated results are shown in Fig. 5. The metastable thickness for Pb films on Si(111) are 1, 3, 6, 8 and 10, which correspond precisely to experimental observations[40]. We also examined the effect of different stacking sequence on the energetics for a two layer and a three layer Pb film. For a two layer Pb film on Si, AB and AC stacking are degenerate in energy. For a three layer Pb film, the difference in total energy between ABC and ACB stacking is also small and less than 0.01 eV per (1×1) unit cell. In addition, we considered three layer Pb films with stacking faults, i.e. ACA and ABA stacking. The formation energy increases by only 0.05 eV per (1×1) unit cell, which is less than the stacking fault energy of 0.12 eV per (1×1) unit cell for a three layer free standing Pb film with a stacking fault. It is more likely for Pb islands on Si(111) to form a stacking fault close to the Pb/Si interface compared to free-standing Pb films.

V. SUMMARY AND CONCLUSIONS

We have presented an *ab initio* simulation of an unprecedented large Pb/Si(111) interface, including structural relaxation and the correct handling of the lattice mismatch. Reducing the number of Pb films on top of the Si substrate, we captured some structural features and their evolution when the Pb film thickness approaches the nano-regime. The Pb overlayer presents notable corrugations of ~ 0.1 Å for the first three Pb layers, those in contact with the Si, and then decays strongly. Beyond the ~ 8 layer, they are essentially flat. The distribution of the corrugation over the slab plane for each Pb layer reveals in fact that the substrate has a great influence over the first Pb films. This effect is progressively lost as we consider outer layers. Interestingly enough, the layers located in the middle section of the overlayer present a more rich and complex corrugation map because of the

competing influence of the substrate on one side, and the end of the Pb overlayer on the other. In terms of energetics, we found metastable thickness for Pb films on top of the Si substrate that agrees well with experimental data.

Acknowledgments

Work at Texas was supported by the Department of Energy for work on nanostructures from grant DE-FG02-06ER46286. We also wish to acknowledge support provided by the Scientific Discovery through Advanced Computing (SciDAC) program funded by U.S. Department of Energy, Office of Science, Advanced Scientific Computing Research and Basic Energy Sciences under award number DESC0008877 on algorithms. Work at Rensselaer Polytechnic Institute was supported by the U. S. Department of Energy under Contract No. DE-SC0002623 and Computational Materials Science Network (CMSN). Computational resources were provided in part by the National Energy Research Scientific Computing Center (NERSC), the Texas Advanced Computing Center (TACC), and the Computational Center for Nanotechnology Innovations (CCNI).

[1] F. K. Shulte, Surf. Sci. **55**, 427 (1976).
[2] B. J. Hinch, C. Koziol, J. P. Toennies, and G. Zhang, Europhys. Lett. **10** 341 (1989).
[3] M. Jalochowski, H. Knoppe, G. Lilienkamp, and E. Bauer, Phys. Rev. B **46**, 4693 (1992).
[4] C.M. Wei and M.Y. Chou, Phys. Rev. B **66**, 233408 (2002).
[5] D. Eom, S. Qin, M.-Y. Chou, and C. K. Shih, Phys. Rev. Lett. **96**, 027005 (2006).
[6] M. Hupalo, S. Kremmer, V. Yeh, L. Berbil-Bautista, E. Abram, and M. C. Tringides, Surf. Sci. **493**, 526 (2001).
[7] A. R. Smith, K.-J. Chao, Q. Niu, and C.-K. Shih, Science **273**, 226 (1996).
[8] L. Gavioli, K. R. Kimberlin, M. C. Tringides, J. F. Wendelken, and Z. Y. Zhang, Phys. Rev. Lett. **82**, 129 (1999).
[9] M. M. Özer, Y. Jia, B. Wu, Z. Y. Zhang, and H. H. Weitering, Phys. Rev. B **72**, 113409 (2005).
[10] C.-S. Jiang, S.-C. Li, H.-B. Yu, D. Eom, X.-D. Wang, P. Ebert, J.-F. Jia, Q.-K. Xue, and C.-K. Shih, Phys. Rev. Lett. **92**, 106104 (2004).
[11] X.-Y. Bao, Y.-F. Zhang, Y. Wang, J.-F. Jia, Q.-K. Xue, X. C. Xie, and Z.-X. Zhao, Phys. Rev. Lett. **95**, 247005 (2005).
[12] J. Slezák, P. Mutombo, and V. Cháb, Phys. Rev. B **60**, 13328 (1999).
[13] H. H. Weitering, D. R. Heslinga, and T. Hibma, Phys. Rev. B **45**, 5991 (1992).
[14] M. Švec, P. Jelínek, P. Shukrynau, C. González, V. Cháb, and V. Drchal, Phys. Rev. B **77**, 125104 (2008).
[15] E. Ganz, I.-S. Hwang, F. Xiong, K. Silva Theiss, and J. Golovchenko, Surf. Sci. **257**, 259 (1991).
[16] L. Seehofer, G. Falkenberg, D. Daboul, and R. L. Johnson, Phys. Rev. B **51**, 13503 (1995).
[17] K. Horikoshi, X. Tong, T. Nagao, and S. Hasegawa, Phys. Rev. B **60**, 13287 (1999).
[18] J. Bardi, N. Binggeli, and A. Baldereschi, Phys. Rev. B **59**, 8054 (1999).
[19] M. Hupalo, V. Yeh, T. L. Chan, C. Z. Wang, K. M. Ho, and M. C. Tringides, Phys. Rev. B **71**, 193408 (2005).
[20] R. T. Tung, Mat. Sci. and Eng. R, **35**, 1 (2001).
[21] L. J. Brillson, Phys. Rev. Lett. **38**, 245 (1977).
[22] G. Ottaviani, K. N. Tu, and J. W. Mayer, Phys. Rev. Lett. **44**, 284 (1980).
[23] S.G. Louie, J.R. Chelikowsky, and M.L. Cohen, Phys. Rev. B **15**, 2154 (1977).
[24] H. Fujitani and S. Asano, Phys. Rev. B **42**, 1696 (1990).
[25] R. G. Dandrea and C. B. Duke, J. Vac. Sci. Technol B **11**, 1553 (1993).
[26] J. R. Chelikowsky, J. Phys. D: Appl. Phys. **33**, R33 (2000).
[27] L. Kronik, A. Makmal, M. L. Tiago, M. M. G. Alemany, M. Jain, X. Huang, Y. Saad, and J. R. Chelikowsky, phys. stat. sol. b **243**, 1063 (2006).
[28] A. Natan, A. Benjamini, D. Naveh, L. Kronik, M. L. Tiago, S. P. Beckman, and J. R. Chelikowsky, Phys. Rev. B **78**, 075109 (2008).
[29] P. Hohenberg and W. Kohn, Phys. Rev. **136**, B864 (1964).
[30] W. Kohn and L. Sham, Phys. Rev. **140**, A1133 (1965).
[31] R. B. Lehoucq, K. Maschhoff, D. Sorensen, and C. Yang, the ARPACK software package, http://www.caam.rice.edu/software/ARPACK/
[32] K. Wu, A. Canning, H. D. Simon, and L.-W. Wang, J. Comput. Phys. **154**, 156 (1999).
[33] Y. Zhou, Y. Saad, M. L. Tiago, and J. R. Chelikowsky, Phys. Rev. E **74**, 066704 (2006).
[34] Y. Zhou, Y. Saad, M. L. Tiago, and J. R. Chelikowsky, J. Comp. Phys. **219**, 172 (2006).
[35] D. M. Ceperley and B. J. Alder, Phys. Rev. Lett. **45**, 566 (1980).
[36] J. P. Perdew and A. Zunger, Phys. Rev. B **23**, 5048 (1981).
[37] N. Troullier and J. L. Martins, Phys. Rev. B **43**, 1993 (1991).
[38] C. M. Wei and M. Y. Chou, Phys. Rev. B **66**, 233408 (2002).
[39] P. B. Howes, K. A. Edwards, J. E. Macdonald, T. Hibma, T. Bootsman, M. A. James, and C. L. Nicklin, Surf. Rev. and Lett. **5**, 163 (1998).
[40] M. C. Tringides and M. Jałochowski, E. Bauer, Phys. Today **60**, 50 (2007).